

BEAM STACKING IN THE RADIAL BETATRON PHASE SPACE*

T. K. Khoe and R. J. Lari
Argonne National Laboratory, Argonne, Illinois USA.

(presented by T. K. Khoe)

A. Introduction

In cases where the emittance of the injector is much smaller than the acceptance of the accelerator, it is advantageous to stack in the betatron phase space. If the pulse length of the injector is much longer than the circumference of the accelerator, multiturn injection is possible with the inherent dilution of the radial phase space density.

In this report, an injection system for accumulating many injector pulses in the radial phase space is discussed. In principle, the stacking could be accomplished without dilution of the phase space density. The method requires the use of bumper magnets which produce a dipole, a quadrupole, and an octupole field. As a result of these perturbation fields, a separatrix is formed with two stable regions separated by an unstable fixed point (Fig. 2).

A fast kicker magnet injects the beam in region I (the smaller loop on the right). The circulating beam of previous injected pulses is in region II (the larger loop). The perturbation fields are adjusted in such a way that at the time of injection, the stable fixed point x_1 coincides with the center of the kicker magnet. After the injection of a pulse is completed, the dipole and octupole fields are adjusted until the separatrix fits tightly around both beams. The quadrupole field is then turned off slowly and the newly injected beam merges with the circulating beam.

The following sections describe the results of analytical and computer studies of the requirements on the bumper fields for injection of many pulses without phase space dilution. Section B gives a derivation of the equations used in the computer program. The computer results are presented in Section C.

B. The Equations of Motion

The bumper magnet fields can be represented in the form

$$b_z(\theta, x, z) = b_0(\theta) + b_1(\theta)x + b_3(\theta)(3xz^2 - x^3)$$

$$b_x(\theta, x, z) = b_1(\theta)z - b_3(\theta)(3x^2z - z^3)$$

where θ denotes the azimuthal location in radians. Substitution of b_z and b_x in the differential equations governing the betatron motion gives

$$\begin{aligned} x'' + \nu_x^2 x &= -\frac{R^2}{B\rho} \left[b_0(\theta) + b_1(\theta)x - b_3(\theta)(x^3 - 3xz^2) \right] \\ z'' + \nu_z^2 z &= \frac{R^2}{B\rho} \left[b_1(\theta)z - b_3(\theta)(3x^2z - z^3) \right] \end{aligned} \quad (1)$$

where primes denote differentiation with respect to θ ; R is the equivalent closed orbit radius and $B\rho$ is the magnetic rigidity of the particle. The bumper magnet occupies only a small fraction of the circumference of the accelerator so that for a practical calculation

$$\frac{R^2}{B\rho} b_n(\theta) = \epsilon_n \delta(\theta)$$

where

$$\epsilon_n = \frac{R^2}{B\rho} \int_{-\pi}^{+\pi} b_n(\theta) d\theta$$

and $\delta(\theta)$ is a periodic delta function, $\delta(\theta+2\pi) = \delta(\theta)$. Substituting this in Eq. (1) results in

$$\begin{aligned} x'' + \nu_x^2 x &= - \left[\epsilon_0 + \epsilon_1 x - \epsilon_3 (x^3 - 3xz^2) \right] \delta(\theta) \\ z'' + \nu_z^2 z &= \left[\epsilon_1 z - \epsilon_3 (3x^2z - z^3) \right] \delta(\theta) \end{aligned} \quad (2)$$

This delta function approximation allows one to use an algebraic transformation from turn to turn instead of the integration of Eq. (1). For a reference point θ_1 radians upstream of the bumper magnet, the relations are:

$$\begin{aligned} x_{n+1} &= x_n \cos \nu_x 2\pi + \frac{x'_n}{\nu_x} \sin \nu_x 2\pi - \frac{U_n}{\nu_x} \sin \nu_x (2\pi - \theta_1) \\ x'_{n+1} &= -\nu_x x_n \sin \nu_x 2\pi + x'_n \cos \nu_x 2\pi - U_n \cos \nu_x (2\pi - \theta_1) \\ z_{n+1} &= z_n \cos \nu_z 2\pi + \frac{z'_n}{\nu_z} \sin \nu_z 2\pi + \frac{V_n}{\nu_z} \sin \nu_z (2\pi - \theta_1) \\ z'_{n+1} &= -\nu_z z_n \sin \nu_z 2\pi + z'_n \cos \nu_z 2\pi + V_n \cos \nu_z (2\pi - \theta_1) \end{aligned} \quad (3)$$

where

$$U_n = \epsilon_0 + \epsilon_1 P_n - \epsilon_3 (P_n^3 - 3P_n Q_n^2)$$

$$V_n = \epsilon_1 Q_n - \epsilon_3 (3P_n^2 Q_n - Q_n^3)$$

$$P_n = x_n \cos \nu_x \theta_1 + \frac{1}{\nu_x} x'_n \sin \nu_x \theta_1$$

$$Q_n = z_n \cos \nu_z \theta_1 + \frac{1}{\nu_z} z'_n \sin \nu_z \theta_1$$

*Work performed under the auspices of the U. S. Atomic Energy Commission.

To find the fixed points in the x, x' plane, set

$$x_{n+1} = x_n, \quad x'_{n+1} = x'_n, \quad z_n \equiv 0, \quad \text{and} \quad z'_n \equiv 0.$$

Equation (3) then reduces to

$$\left[\frac{x_n \cos \nu_x \pi}{\cos \nu_x (\pi - \theta_1)} \right]^3 - \left[\frac{\epsilon_1 + 2\nu_x \tan \nu_x \pi}{\epsilon_3} \right] \times \left[\frac{x_n \cos \nu_x \pi}{\cos \nu_x (\pi - \theta_1)} \right] - \frac{\epsilon_0}{\epsilon_3} = 0 \quad (4)$$

$$x'_n = -\nu_x x_n \tan \nu_x (\pi - \theta_1)$$

which give the fixed point coordinates

$$x_{nk} = 2r \frac{\cos \nu_x (\pi - \theta_1)}{\cos \nu_x \pi} \cos \left(\frac{\alpha + 2(k-1)\pi}{3} \right) \quad (5)$$

$$x'_{nk} = -2\nu_x r \frac{\sin \nu_x (\pi - \theta_1)}{\cos \nu_x \pi} \cos \left(\frac{\alpha + 2(k-1)\pi}{3} \right),$$

for $k = 1, 2, 3$, and where r and α are given by

$$r = \sqrt{\frac{\epsilon_1 + 2\nu_x \tan \nu_x \pi}{3\epsilon_3}} \quad \text{and}$$

$$\cos \alpha = \frac{\epsilon_0}{2\epsilon_3} \sqrt{\left(\frac{3\epsilon_3}{\epsilon_1 + 2\nu_x \tan \nu_x \pi} \right)^3}$$

Two of the fixed points are stable; one unstable.

C. The Computer Facilities and Calculations

The recursion equations (3) have been programmed in the Fortran language for the SEL-810A computer. This has an 8K-word memory, teletype input, line printer output, a CRT display, and a 1000K-word disc pack. The CRT has an 8 x 8-cm storage screen with a 256 x 256 matrix of points. Sense switches on the computer can be set to select input variables on the teletype.

The values of x_n, x'_n, z_n, z'_n are calculated for the given values of the parameters $\epsilon_0, \epsilon_1, \epsilon_3, \theta_1, \nu_x$, and ν_z , starting from the initial points $(x_0, x'_0) (z_0, z'_0)$. The calculated points $(x_n, x'_n) (z_n, z'_n)$ trace a trajectory in phase space. The points are close together in the neighborhood of the fixed points. Figure 1 shows a typical trace on the CRT.

In this case, (x_0, x'_0) is chosen very close to the unstable fixed point so that the points (x_n, x'_n) practically trace a separatrix. The upper curve shows the stable z-motion. Figure 2 shows the same trajectory for $\theta_1 = \pi$. It is not difficult to see from Eq. (5) that, in this case, the fixed points lie on the x-axis.

In addition, the computer program calculates for $z_0 = 0, z'_0 = 0$, the fixed points, the areas of the two regions, and their ratio. Table I gives the values of these quantities as a function of ϵ_0, ϵ_1 , and ϵ_3 for $\nu_x = 0.84$ and $\theta_1 = \pi$.

The injection of 11 sets of pulses from the booster into the ZGS will be used to illustrate the whole procedure.

The equilibrium orbit is shifted to the location of the kicker magnet ($x = x_k$) and the first set of pulses is injected to fill all RF buckets. After this injection is completed, the equilibrium orbit is moved to $x = 0$ and the bumper magnets turned on (first ϵ_0 and ϵ_3 , then ϵ_1). Figure 3 top shows the beam boundary in the radial phase space and a trajectory for larger amplitude.

For $\epsilon_1 = 0$, there is no separatrix in the region of interest. The beam center is slightly displaced because of the dipole field ϵ_0 . For ϵ_1 satisfying the condition

$$\frac{\epsilon_0}{2\epsilon_3} \sqrt{\left(\frac{3\epsilon_3}{\epsilon_1 + 2\nu_x \tan \nu_x \pi} \right)^3} = 1 \quad (6)$$

the unstable fixed point and the stable fixed point of region I coincide (Fig. 3 middle). Figure 3 bottom shows the two-loop separatrix for $\epsilon_1 = 1.13$ and the same values of ϵ_0 and ϵ_3 . The stable fixed point of region I is at the kicker magnet ($x_{SI} = x_k$). The second set of pulses is then injected and the dipole field turned off (Fig. 4 top). The shrinking of the separatrix by turning off slowly the quadrupole field ϵ_1 is shown in Fig. 4.

Prior to injecting the third set of pulses, ϵ_0 and ϵ_3 are reset to the values of Fig. 3, followed by turning on ϵ_1 . After the injection, ϵ_3 is increased until the separatrix fits tightly around both beams. The chosen value of ϵ_0 gives an area ratio of 2:1. The injected and circulating beams merge when ϵ_1 is turned off. The steps of Fig. 3 are repeated prior to injecting the fourth and subsequent set of pulses. The values of ϵ_0 and ϵ_3 are adjusted after each injection to give a tight fit of the separatrix around both beams before turning ϵ_1 off. Figure 5 shows the shrinking of the separatrix after injecting 11 sets of pulses. The ratio of the region areas of the last separatrix is ten. The merging of the regions into one of the same phase space area is shown in Fig. 6.

D. Conclusions

Although the computer results and the phase space trajectories described in the preceding section pertained to injection from a booster synchrotron into the ZGS, the method can be applied to other accelerators provided the radial acceptance is much larger than the beam emittance. For more details of this method, see Ref. 1.

E. References

¹T. K. Khoe and R. J. Lari "Beam Stacking in the Radial Betatron Phase Space," Accelerator Division Internal Report TTK/RJL-1, Argonne Nat'l. Laboratory, August 9, 1971.

Table I

ϵ_0 (cm)	ϵ_1	ϵ_3 (cm ⁻²)	A_I (cm ²)	A_{II} (cm ²)	A_{II}/A_I	x_{sI} (cm)	x_{sII} (cm)	x_u (cm)
.1811	1.13	.00292	27.83	54.84	1.971	9.048	-10.060	1.013
.3200	1.13	.00226	26.37	80.81	3.064	9.881	-11.701	1.820
.4278	1.13	.00184	26.53	107.3	4.044	10.662	-13.130	2.468
.5179	1.13	.00155	27.26	133.8	4.907	11.394	-14.417	3.023
.6113	1.13	.00134	26.80	162.2	6.054	12.005	-15.620	3.616
.6900	1.13	.00118	26.95	188.9	7.010	12.603	-16.725	4.123
.7575	1.13	.00106	26.99	215.5	7.984	13.144	-17.707	4.563
.8235	1.13	.000965	26.82	240.4	8.964	13.616	-18.618	5.003
.8858	1.13	.000883	26.77	267.1	9.978	14.903	-19.514	5.421

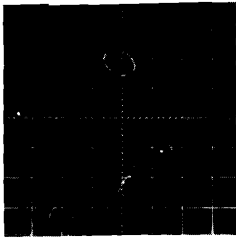


Figure 1

$\theta_1 = 4$ radians
 $\epsilon_0 = 0.0265$ cm
 $\epsilon_1 = 1.13$
 $\epsilon_3 = 0.33$ cm⁻²

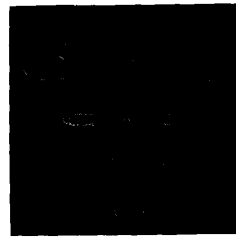


Figure 4

$\epsilon_0 = 0.0$ cm
 $\epsilon_1 = 1.13$ (top)
 $\epsilon_1 = 1.00$
 $\epsilon_1 = 0.80$
 $\epsilon_1 = 0.00$ (bottom)
 $\epsilon_3 = 0.0004$ cm⁻²

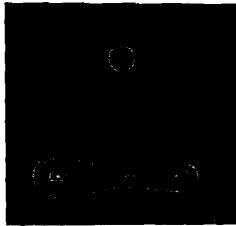


Figure 2

$\epsilon_0 = 0.0265$ cm
 $\epsilon_1 = 1.13$
 $\epsilon_3 = 0.33$ cm⁻²



Figure 5

$\epsilon_0 = 0.8858$ cm
 $\epsilon_1 = 1.13$
 $\epsilon_3 = 0.0004$ (top)
 $\epsilon_3 = 0.0006$
 $\epsilon_3 = 0.000883$ (bot) } cm⁻²



Figure 3

$\epsilon_0 = 0.1811$ cm
 $\epsilon_1 = 0.0$ (top)
 $\epsilon_1 = 0.96815$ (middle)
 $\epsilon_1 = 1.13$ (bottom)
 $\epsilon_3 = 0.0004$ cm⁻²



Figure 6

$\epsilon_0 = 0.8858$ cm
 $\epsilon_1 = 1.13$ (top)
 $\epsilon_1 = 1.09081$ (middle)
 $\epsilon_1 = 0.00$ (bottom)
 $\epsilon_3 = 0.000883$ cm⁻²

NOTE: For all figures, $\nu_x = 0.84$, $\nu_z = 0.79$, and $\theta_1 = \pi$, except Fig. 1.

DISCUSSION

M. BARTON : Your model idealises the machine. Have you examined the effect of imperfections on this scheme ?

T. KHOE : The dipole and quadrupole error fields are much smaller than the introduced dipole and quadrupole fields. We have considered the effect of small tune changes. We did not consider sextupole error fields.

L.C. TENG : I would suggest that this scheme is very useful for a storage ring when it is desirable to stack the beam in the betatron oscillation phase space instead of the phase oscillation space.

T. KHOE : In practice this stacking is only possible for $\frac{\text{acceptance}}{\text{emittance}} > 4$.